

## SALT DAMAGE ON THE WALL PAINTINGS OF THE FESTIVAL TEMPLE OF THUTMOSIS III, KARNAK TEMPLES COMPLEX, UPPER EGYPT. A CASE STUDY

Hussein MAREY MAHMOUD<sup>1\*</sup>, Nikolaos KANTIRANIS<sup>2</sup>, John STRATIS<sup>3</sup>

<sup>1</sup>) Department of Conservation, Faculty of Archaeology, Cairo University, Giza, Egypt.

<sup>2</sup>) Department of Mineralogy-Petrology-Economic Geology, Aristotle University, Thessaloniki, Greece.

<sup>3</sup>) Laboratory of Analytical Chemistry, Aristotle University, Thessaloniki, Greece.

### Abstract

*The present study aims to characterize the main deterioration mechanisms affecting the wall painting of the festival temple of Thutmose III, in the Karnak temples complex, Upper Egypt. Several salt encrustations were observed on the painted surfaces, exhibiting different degrees and forms of decay. The morphology and the microanalysis of the contained mineral phases were studied using scanning electron microscopy together with an energy dispersive X-ray analysis system (SEM-EDS). The mineralogical characterization was performed using the X-ray powder diffraction method (XRPD). The climatic conditions of the area play an important role in the crystallization/recrystallization cycles of salts, which exerts additional pressure, by producing cracking, powdering and flaking, in addition to pulverization of the pictorial layers. The results showed that sodium chloride (halite, NaCl) is the predominant salt species affecting in the site. Furthermore, other salt minerals, such as sylvite (KCl), niter (KNO<sub>3</sub>), natron (Na<sub>2</sub>CO<sub>3</sub>·10H<sub>2</sub>O), thenardite (Na<sub>2</sub>SO<sub>4</sub>), gypsum (CaSO<sub>4</sub>·2H<sub>2</sub>O), anhydrite (CaSO<sub>4</sub>) and bassanite (CaSO<sub>4</sub>·0.5H<sub>2</sub>O) were also found. The obtained results allowed us to determine the main deterioration factors and may be used when applying a conservation plan.*

**Keywords:** Karnak temples complex; Wall paintings; Salt damage; XRPD; SEM-EDS.

### Introduction

The Karnak temples are considered to be among the largest monuments in the world. There are approximately 20 minor temples at Karnak and approximately 30 pharaohs contributed to the buildings, enabling Karnak to reach a size, complexity and diversity not seen elsewhere in the world (situated on 100 ha of land) [1]. Karnak is located about 2.5 km in north of Luxor and about 670 km south of Cairo. It is dated back to the New Kingdom, the 18th dynasty (c.1540–1292 BC) until the late period of Egypt, although new excavations were dated back to the Old Kingdom (c. 2575–2465 BC). The relatively complete festival temple of Thutmose III lies beyond the central court, which retains some of the most interesting and unusual features to be found at Karnak. The festival temple of Thutmose III is spacious and elegant, 44 meters wide and 10 deep. The roof is supported by 20 columns in two rows and 32 square pillars on the sides [2]. The wall paintings of the festival temple of Thutmose III are carved with raised and sunken reliefs and painted with religious scenes and inscriptions. The chromatic palette used in the decorations of the temple was identified using different analytical techniques (OM, SEM-EDS, FTIR,  $\mu$ -Raman spectroscopy) and it revealed use of inorganic

\* Corresponding author: marai79@hotmail.com, +20.239.848641

minerals (mainly yellow and red ochre) and synthetic pigments e.g. Egyptian blue (cuprorivaite) [3].

The main objective of this study was to characterize some salt encrustations formed on the painted surfaces of the festival temple of Thutmose III, in the Karnak temple complex (Fig. 1).



**Fig. 1.** Crystallization of different salts on the painted surfaces of the festival temple of Thutmose III, Karnak complex temples. The locations of the collected salt samples are also shown.

The obtained results will help understanding the weathering mechanisms affecting the site and consequently choose the suitable materials for conservation. The main building materials used in the temples are sandstones, so-called "Nubian Sandstone", collected from the Gebel el-Silsila area, in South-Western Egypt (about 160km south of Luxor, 50km north of Aswan) [4]. According to A. Saleh et al [5], the sandstone in the Karnak temples consists mainly of quartz ( $\alpha$ -SiO<sub>2</sub>), with traceable amounts of kaolinite (Al<sub>2</sub>Si<sub>2</sub>O<sub>5</sub>(OH)<sub>4</sub>), haematite ( $\alpha$ -Fe<sub>2</sub>O<sub>3</sub>), albite (NaAlSi<sub>3</sub>O<sub>8</sub>) and oligoclase. Many papers focused on the study of the mineralogical and geochemical properties of the building materials and on the weathering mechanisms affecting the Karnak temples and other stone monuments in Upper Egypt [4-8]. The crystallization of salts in porous building materials is a challenging problem for conservation projects of mural paintings and stone monuments. Practically, all walls contain soluble salts; either dispersed within the porous materials or concentrated locally [9]. There are several sources of inorganic salts in wall paintings. Perhaps the most obvious are the materials used for the artwork itself; stones, bricks, plaster and mortar can all contain inorganic salts [10]. While such porous materials are drying, salt crystallization may occur on the surface (that is, efflorescence) or just beneath the surface, where it may cause structural damage, for example, delamination, surface chipping, or disintegration, with consequent loss of detail [11]. Wetting and drying is an inevitable part of the process leading to salt crystallization, causing

damage to stonework, even if the wetting phase sometimes involves water vapors rather than liquid water [12]. Salts produce destructive effects, in certain conditions; some salts may crystallize or re-crystallize into different hydrates, which occupy a larger space and exert additional pressure, producing cracking, powdering and flaking [13].

#### ***Highlighting the weathering mechanisms affecting the site***

The main weathering factors affecting the site are the physiochemical factors resulting from the penetration of the groundwater - mainly from the ancient sacred lake located in the temple - which reacts with the lower parts of the stone blocks causing several damages in the area close to the ground surface, due to the action of capillary water [14]. The problem at Karnak is mainly attributed to the dramatic rise of the water level and it is not directly linked to the rise in groundwater cause by the Aswan dam. Rising close to the ground surface, water adversely affected the stone structure of the temple [15]. The main reasons for the water rise are seepage from land reclamation areas to the east, and leakages from poor sewer structures in the increasingly expanding housing areas. On the other hand, the Luxor climate is rated between arid and semi-arid. The monthly average of air temperature ranges between 12 and 32 °C. The maximum relative humidity (RH %) reaches 50% in December and 29% in August, while average rainfall ranges from 0.01 to 0.2 mm. The evaporation rates are lowest in January (2.5 mm/day) and highest in June (9.4 mm/day), and the average wind velocity ranges between 3.7 and 21.1km/h. The extensive changes in air temperature favors the crystallization/re-crystallization cycles of salts, causing exfoliation, blistering, disintegration and the formation of many salt encrustations on the painted surfaces. It is well known that every visitor to the archaeological site produces series of variations in the interior microclimate, due to his own metabolism [16]. For instance, an individual walking slowly (3.2 km/hr) in an environment of 15 °C develops a heat power of approximately 200W, releasing 100g of water vapors and 100g of CO<sub>2</sub>. It is estimated that an individual releases in the environment several hundred thousand particles (including 1,000 to 10,000 germs) per minute. Obviously, there are variations depending on individuals [17].

### **Materials and methods**

#### ***a. Sampling***

Micro-samples of the different salt encrustations were carefully collected from several locations on the walls, especially from the friable layers, using a metallic scalpel. A small amount of powder was scraped off from the hard crusts. The collected samples were crushed and milled in the agate mortar in order to avoid contamination. The powder of the samples was analyzed to determine their chemical and mineralogical composition.

#### ***b. Scanning electron microscopy (SEM-EDS)***

Scanning electron microscopy (SEM) provides information about mineral morphology, crystal features, and chemical composition. In this study a JEOL JSM-840A scanning electron microscope equipped with energy dispersive X-ray (EDS), Oxford ISIS 300 micro analytical system was used to investigate the weathered layers. Operating conditions were: accelerating voltage 20kV, probe current 45nA and counting time 60 seconds, with ZAF correction being provided on-line.

#### ***c. X-ray powder diffraction analysis (XRPD)***

The collected salt samples were ground into powder in agate mortar and studied by X-ray powder diffraction analysis (XRPD), in order to determine their mineralogical composition. XRPD measurements were performed using a Phillips PW1710 diffractometer with Ni-filtered

Cu- $k_{\alpha}$  radiation. The samples were scanned over the 3–63° 2 $\theta$  interval at a scanning speed of 1.2°/min. Quantitative estimates of the abundance of the mineral phases were derived from the XRPD data, using the intensity of a certain reflection, the density and the mass absorption coefficient for Cu- $k_{\alpha}$  radiation for the minerals present. Corrections were made using external standard mixtures of minerals. The detection limit of the method was  $\pm 2\%$  w/w.

## Results and discussion

The quantitative EDS microanalysis (compound %) and the mineralogical composition (w/w %) of the studied salt samples are given in Tables 1 and 2.

**Table 1.** Quantitative EDS microanalysis (compound %) of the damaged layers

Sample	Na <sub>2</sub> O	MgO	Al <sub>2</sub> O <sub>3</sub>	SiO <sub>2</sub>	SO <sub>3</sub>	K <sub>2</sub> O	CaO	TiO <sub>2</sub>	Fe <sub>2</sub> O <sub>3</sub>	Cl
<i>Ks.1</i>	12.50	–	2.11	6.32	33.27	13.87	15.57	1.43	2.20	9.65
<i>Ks.2</i>	0.87	–	4.29	29.33	22.24	6.04	24.74	3.23	5.10	1.71
<i>Ks.3</i>	32.34	–	1.20	9.22	12.98	0.44	7.29	0.87	–	31.91
<i>Ks.4</i>	22.94	2.52	4.67	26.72	14.22	2.36	9.23	1.86	4.53	7.34

**Table 2.** Mineralogical composition (w/w %) of the studied samples

Component/sample	Surface deposit ( <i>Ks.1</i> )	Salt layer ( <i>Ks.2</i> )	Thin salt layer ( <i>Ks.3</i> )	Thin salt layer ( <i>Ks.4</i> )
Halite	54	21	84	80
Gypsum	–	–	–	14
Bassanite	2	3	4	4
Anhydrite	–	–	5	–
Sylvite	–	9	–	–
Niter	–	–	2	–
Natron	–	3	–	–
Quartz	2	2	3	2
Thenardite	–	6	–	–
Calcite	38	54	–	–
Dolomite	2	–	–	–
Micas	–	2	–	–
K-feldspar	–	–	2	–
Plagioclase	2	–	2	–

### *a. Morphology and microanalysis*

Figure 2 displays SEM micrographs obtained for the salts layers. SEM image of a surface salt deposit (sample *Ks.1*) taken from a higher area in the murals shows a dense coat of halite crystals which covers the pores of the stone (Fig. 2a).

An EDS microanalysis of the sample showed that S and Cl are the major ions contained, while Ca, K, Na and Si are secondary elements. Traces of Al, Fe and Ti were also found. A SEM image of a salt layer (sample *Ks.2*) taken from a wall in the main court of the temple shows the crystallization of bristly crystals of halite. Prism and plates-like crystals of gypsum were also detected (Fig. 2b). EDS microanalysis of the sample showed that Ca, S and Si are the major ions contained, with minor elements of Al, Na, Cl and K, while traces of Fe and Ti were also detected. A SEM image of a thin salt layer (sample *Ks.3*) taken from a side room of the temple shows fluffy and hair-like crystals of halite (Fig. 2c). EDS microanalysis of the sample showed that Cl and Na are the major ions contained, with minor elements of Ca, S and Si, while traces of Al were also determined. A SEM image of a salt layer (sample *Ks.4*) crystallized on a raised relief in a room on the right side of the court with columns shows waxy

and hollow-faced coats of halite crystals, completely covering the stone surface (Fig. 2d). EDS microanalysis of the sample showed that Si, Na and Cl are the major ions contained, while Ca and S were detected as secondary elements. Traces of K, Al, Mg, Fe and Ti were also determined.

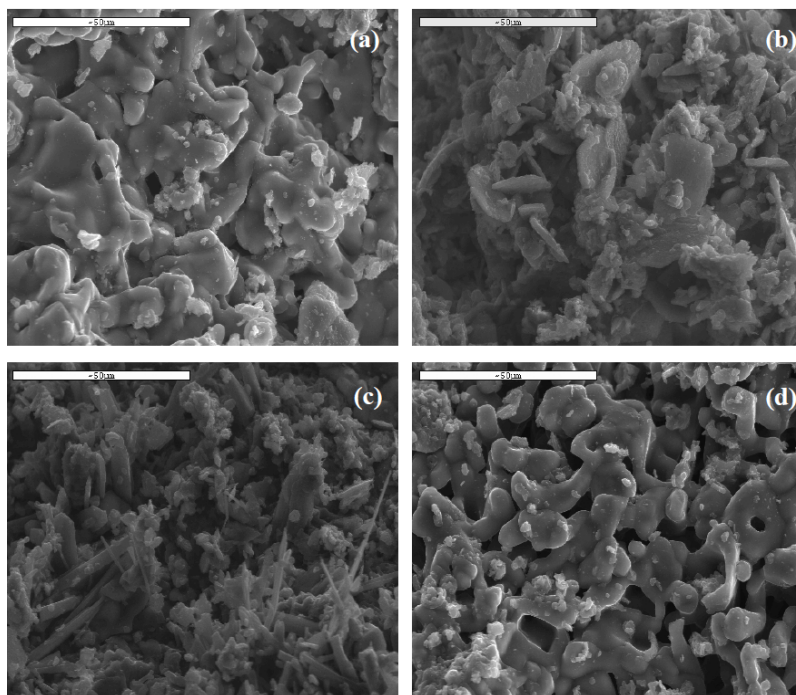


**Fig. 2.** SEM micrographs show: a) a dense coat of halite salts, b) the crystallization of prism and plate-like crystals of gypsum, c) fluffy and hair-like crystallization of salts, d) waxy and hollow-faced layers of halite cover the stone surface.

### ***b. The mineralogical characterization***

Representative XRPD patterns of the studied salt samples are given in Figure 3. XRPD patterns of the surface salt deposit (sample *Ks.1*) show that the sample consists mainly of halite (NaCl, 54%) and calcite (CaCO<sub>3</sub>, 38%).

Certain amounts of bassanite (CaSO<sub>4</sub>·0.5H<sub>2</sub>O, 2%), quartz (SiO<sub>2</sub>, 2%), dolomite [CaMg(CO<sub>3</sub>)<sub>2</sub>, 2%] and plagioclase (NaAlSi<sub>3</sub>O<sub>8</sub>, 2%) were also detected (Fig. 3a). XRPD patterns of the salt layer (sample *Ks.2*) show that the sample consists mainly of calcite (54%) with minor amounts of halite (21%), sylvite (KCl, 9%), thenardite (Na<sub>2</sub>SO<sub>4</sub>, 6%), bassanite (3%), natron (Na<sub>2</sub>CO<sub>3</sub>·10H<sub>2</sub>O, 3%), micas (2%) and quartz (2%) (Fig. 3b). XRPD patterns of the thin salt layer (sample *Ks.3*) show that the sample consists mainly of halite (84%). Certain amounts of bassanite (4%), quartz (3%), anhydrite (CaSO<sub>4</sub>, 5%), K-feldspar (KAlSi<sub>3</sub>O<sub>8</sub>, 2%), plagioclase (2%) and niter (KNO<sub>3</sub>, 2%) were also detected. XRPD patterns of the thin salt layer (sample *Ks.4*) show that the sample consists mainly of halite (80%) and gypsum (CaSO<sub>4</sub>·2H<sub>2</sub>O, 14%), with minor amounts of bassanite (4%) and quartz (2%).

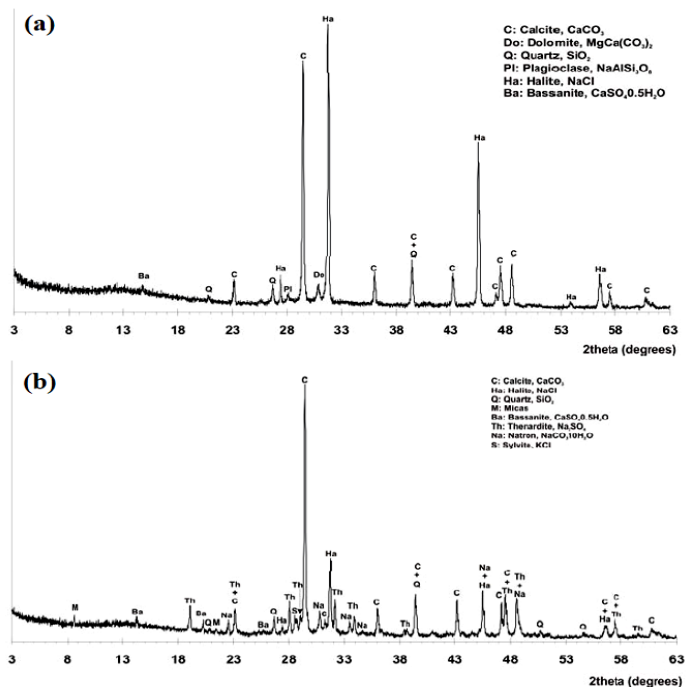


**Fig. 3.** Representative XRPD patterns of: a - a surface salt deposit covers the wall paintings (sample Ks1), b - a salt layer (sample Ks2).

**c. Salt crystallization**

The mineralogical analyses using XRPD analysis of the damaged layers have shown that the salt layers consist mainly of halite and phases of sulphates (gypsum, anhydrite and bassanite). Other salts of sylvite, niter, natron and thenardite were also detected. On the higher areas of the mural paintings especially in the areas close to the ceiling, white veils of gypsum are formed. In these cases, gypsum crystallized in small particles and the mechanism of their formation at this higher location is correlated with the presence of hygroscopic salts - such as halite and sylvite in our case study - which would allow the slow migration of gypsum to this location [18, 19]. A. Ismail et al [20] reported that the total dissolved salts of water in the sacred lake of the Karnak temples complex is relatively high (780mg/L) and the groundwater salinity ranges from 524 to 1,363 mg/L, increasing from the edges of the Quaternary Aquifer towards the River Nile in the same direction as the groundwater flow. According to G. El-Bayomi [14], the continuous migration of the water from the sacred lake and the seepage from the cultivated lands near the temple occurs due to evaporation into two ways: a) the dissolving of salts reduces the strength of stone as the cementing agent is partly removed, and b) the more spectacular damage takes place at the surface where the dissolved salts re-crystallized and their expansion causes deterioration.

On the other hand, the old restoration attempts using gray Portland cements could be affected by capillary rise of saline water which led to sandstone backing and formed different salt encrustations [21]. Moreover, the fine plasters used in the construction of the mural paintings are usually based on gypsum and calcite, which could be dissolved and re-crystallized depending on the environmental conditions. Gypsum has a low solubility (257.5mg/100g water at 20 °C) so it is crystallized at high levels of humidity [22], and the continuous supply of the groundwater allows gypsum formation. Bassanite was detected in all

the studied samples. Transformation of gypsum into bassanite or anhydrite occurs at relatively high ambient temperatures and/or high brine salinities (e.g., 45 °C at  $a_{\text{H}_2\text{O}}$  0.88) [23]. The dehydration of gypsum to hemi-hydrate requires a lower relative humidity than the dehydration of gypsum to anhydrite. Although gypsum also starts to dehydrate to form the hemi-hydrate (bassanite) at 42 °C, only in few instances has this salt been found in nature, such as in the semiarid gypsum deposits in south Tunisia, where it formed due to the extreme conditions in this area, with temperatures reaching 70 or 80 °C and with very low humidity [18]. However, the dehydration of gypsum is extremely slow below 42 °C and it is affected by the nature of other materials present in the system, as in the case of monuments [24]. In addition, the presence of solutions of other salts such as  $\text{KNO}_3$  and  $\text{NaCl}$  which were detected in some of the studied samples could lead to the dehydration of gypsum as a result of the lower water vapor pressure of these solutions. The deterioration caused by gypsum and any other non-hydrating salts to stone and related building materials is a result of its crystallization within the porous material matrix. The damage mechanism originates in the stress generated during the growth of the gypsum crystals, generally called crystallization pressure. Because of its low mobility, gypsum tends to accumulate in large pores, and in an enhanced moisture retention environments, thus facilitating gypsum re-crystallization and the development of larger crystals [25]. Halite was identified in all the studied samples. Halite is one of the most abundant and ubiquitous element [26] and it is a natural impurity in the Egyptian soil and a common mineral in marine sediments.

Chlorides are known to accelerate the hydration process of the Portland cement used in old restorations of the temple and that led to salt crystallization. Sylvite and niter were detected in some of the studied samples (samples *Ks.2* and *Ks.3*) and that probably resulted from the migration of potassium ions from the cultivated lands close to the temple. Moreover, the potassium feldspar found in the sandstone composition of the temple could provide a minor source of potassium ions, which, when reacted with chloride ions, give rise to the formation of sylvite [5]. Highly hydrated salts such as natron were also detected in our case. This was probably due to high alkaline reaction of the penetrating salt solution with the lime-based plaster layers in the temple. Thenardite was also detected in some samples (sample *Ks.2*). The reaction of the Portland cement with the groundwater could be the source of this salt. Thenardite tends to precipitate inside the solution creating subflorescence within the pores of the stone, while halite tends to precipitate at the air solution interface, preferentially creating harmless efflorescences growing on the stone surface.

According to C. Rodriguez-Navarro et al [27], the precipitation of thenardite rather than mirabilite ( $\text{Na}_2\text{SO}_4 \cdot 10\text{H}_2\text{O}$ ) may be the culprit in damages caused by sodium sulphate, particularly in situations of constant capillary rise.

## Conclusion

The results showed that the deterioration processes of the mural paintings of the festival temple of Thutmosis III, in Karnak, are mainly caused by salt crystallization. Salts play another role in the deterioration process of stone materials. By increasing their thermal expansion coefficient they consequently enhance the decay mechanisms connected with temperature fluctuations [28]. That can produce expansive stresses and internal microfracture, in addition to blistering, micro and macro cracks and pulverizations of the paint layers. The results have shown that the main salts affecting the site are: sodium chloride (halite,  $\text{NaCl}$ ), as the predominant salt affecting the site. Salts of sylvite ( $\text{KCl}$ ), niter ( $\text{KNO}_3$ ), natron

( $\text{Na}_2\text{CO}_3 \cdot 10\text{H}_2\text{O}$ ), thenardite ( $\text{Na}_2\text{SO}_4$ ), gypsum ( $\text{CaSO}_4 \cdot 2\text{H}_2\text{O}$ ), anhydrite ( $\text{CaSO}_4$ ) and bassanite ( $\text{CaSO}_4 \cdot 0.5\text{H}_2\text{O}$ ) were also detected. The morphological study of the salt samples, performed by SEM, has shown that different forms of salt crystallization occurred, depending mainly on the salt type itself, the building material, and the surrounding environmental conditions.

It was clear from the site investigations and the study of different salt encrustations that the salt damage resulted from:

- The penetration of the groundwater and mainly from the sacred lake situated inside the temple, the water seepage from land reclamation areas, and leakages from poor sewage conditions in the increasingly expanding housing areas. That water reacts with the components of the wall paintings forming different salt encrustations;
- Wetting and drying cycles favor crystallization of many salt phases inside the pores of stone or into hard crusts.

The long-term environmental monitoring of the site, in association with further investigation of additional samples may prove important in establishing suitable conservation plans to stop or minimize the decay.

### Acknowledgements

H.H. Marey Mahmoud would especially like to thank the State Scholarships Foundation (IKY) of Greece for the financial support of his PhD thesis. The authors would like to thank Mr. S. Oikonomidis, School of Geology, Aristotle University for SEM investigation.

### References

- [1] B. Alexander, **History of Egyptian Architecture, The Empire (The New Kingdom) From the Eighteenth Dynasty to the End of the Twentieth Dynasty 1580-1085 B.C.** University of California Press, 1968.
- [2] J. Kamil, **LUXOR: A Guide to Ancient Thebes** (second edition), London, 1976, p. 54.
- [3] H. Marey Mahmoud, *Study of the chromatic changes of the ancient pigments in some wall paintings in Egypt and the procedures of conservation*, **PhD. Thesis**, Postgraduate Interdepartmental Program on: Protection, Conservation & Restoration of Cultural Monuments, Faculty of Engineering of Aristotle University of Thessaloniki, 2009.
- [4] B. Fitzner, K. Heinrichs, D. La Bouchardiere, *Weathering damage on Pharaonic sandstone monuments in Luxor-Egypt*, **Building and Environment**, **38** (9-10), 2003, pp. 1089–1103.
- [5] S.A. Saleh, F.M. Helmi, M.M. Kamal, A.E. El Banna, *Study and consolidation of sandstone: Temple of Karnak, Luxor, Egypt*, **Studies in Conservation**, **37** (2), 1992, pp. 93–104.
- [6] T.C. Billard, G. Burns, *Mechanisms of Stalinitization of great Temples in Luxor area*, **Journal of the Society for the Study of Egyptian Antiquities**, **10**, 1980, pp. 243–249.
- [7] I. Badawy, A. Abdel Moniem, *Environmental deterioration of Karnak Temples, Luxor, Upper Egypt*, **Bulletin of Faculty of Engineering**, Assiut University, Egypt, **27** (1), 1999, pp. 273–302.

- [8] M.M. Abd El Hady, *The deterioration of Nubian sandstone in the Ptolemaic Temples in Upper Egypt*, **Proceedings of the 9th International Congress on the Deterioration and Conservation of Stone**, 2, 19-24 June, Venice, Italy, 2000, pp. 783–792.
- [9] A. Arnold, K. Zehnder, *Monitoring Wall Paintings Affected by Soluble Salts*, In the *Conservation of Wall Paintings*, **Proceedings of a Symposium organized by the Courtauld Institute of Art and the Getty Conservation Institute**, 13-16 July, London, 1987, pp. 103–135.
- [10] E. Kotulanová, P. Bezdička, D. Hradil, J. Hradilová, S. Švarcová, T. Grygar, *Degradation of lead-based pigments by salt solutions*, **Journal of Cultural Heritage**, **10**, 2009, pp. 367–378.
- [11] L. Pel, H. Huinink, K. Kopinga, *Ion transport and crystallization in inorganic building materials as studied by nuclear magnetic resonance*, **Applied Physics Letters**, **8** (5), (2002), pp. 2893–2895.
- [12] D.B. Honeyborne, *Weathering and decay of masonry*, **Conservation of Building & Decorative Stones** (second edition), (editors Ashurst J., Dimes F.G.), Butterworth-Heinemann, 1998, pp. 153–178.
- [13] C. Rodriguez-Navarro, E. Doehne, *Salt Weathering: Influence of Evaporation rate, super saturation and crystallization Pattern*, **Earth Surface Processes and Landforms**, **24**, 1999, pp. 191–209.
- [14] G.M. EL-Bayomi, *The Geomorphological Hazards in the Archaeological Area West of Qena Bend*, **Journal of Applied Sciences Research**, **3** (3), 2007, pp. 175–184.
- [15] C. Tortajada, *International Workshop on Hydro politics and impacts of the Aswan High Dam*, **Conference Report, Ministry of Water Resources and Irrigation of Egypt**, Cairo, 14 February, 2007.
- [16] M. Hoyos, V. Soler, J.C. Canaveral, S. Sánchez-Moral, E. Sanz-Rubio, *Microclimatic Characterization of a karstic Cave: Human impact on Micro Environmental Parameters of a Prehistoric Rock Art Cave (Candamo Cave, northern Spain)*, **Environmental Geology**, **33** (4), 1998, pp. 231–242.
- [17] P. Diaz-Pedregal, A. Diekmann, *How to reconcile Archaeological Site Protection and Visitor Accessibility?*, **APPEAR Position Paper**, **2**, 2004, pp. 1–9.
- [18] A.E. Charola, J. Pühringer, M. Steiger, *Gypsum: a review of its role in the deterioration of building Materials*, **Environmental Geology**, **52**, 2007, pp. 339–352.
- [19] K. Zehnder, *New aspects of decay caused by crystallization of gypsum*, **Conservation of stone and other materials** (ed. Thiel M.-J.). Vol. I, London, 1993, pp. 107–114.
- [20] A. Ismail, N.L. Anderson, J. David Rogers, *Hydro geophysical Investigation at Luxor, Southern Egypt*, **Journal of Environmental and Engineering Geophysics**, **10** (1), 2005, pp. 35–49.
- [21] G. Martinet, F.X. Deiyo, A. Le Roux, *Nature and weathering of the mortars used in the restoration of the Temple of Amon at Karnak (in French)*, **Bulletin de Liaison du Laboratoire des Ponts et Chaussees**, **182**, 1992, pp. 21–26.
- [22] V. Galvan Iopis, A. Mastomas, E. Gilbenso, *Conditions that influence the position and crystallization of salts*, **Proceedings of the 7th International Congress on Deterioration and Conservation of Stone**, 24–29 October 1992, Lisbon, pp. 895–904.
- [23] F. Mees, M. De Dapper, *Vertical variations in bassanite distribution patterns in near-surface sediments, southern Egypt*, **Sedimentary Geology**, **181**, 2005, pp. 225–229.

- [24] A.E. Charola, S.A. Centeno, *Analysis of gypsum-containing lime mortars: Possible errors due to the use of different drying conditions*, **Journal of American Institute for Conservation (JAIC)**, **41**, 2002, pp. 269–278.
- [25] M. Steiger, *Crusts and salts*, **Air pollution reviews, Vol 2. The effects of air pollution on the built environment** (ed. P. Brimblecombe), Imperial College Press, London, 2003, pp. 133–181.
- [26] B. Lubelli, R.P.J. van Hees, C.J.W.P. Groot, *Sodium chloride crystallization in a “salt transporting” restoration plaster*, **Cement and Concrete Research**, **36**, 2006, pp. 1467–1474.
- [27] C. Rodriguez-Navarro, E. Doehne, E. Sebastian, *How does sodium sulphate crystallize? Implications for the decay and testing of building materials*, **Cement and Concrete Research**, **30**, 2000, pp. 1527–1534.
- [28] M. Al-Naddaf, *The effect of salts on thermal and hydric dilatation of porous building stones*, **Archaeometry**, **51** (3), 2009, pp. 495–505.
- 

*Received: July 1, 2010*

*Accepted: July 28, 2010*